Journal of CO2 Utilization 56 (2022) 101822

Contents lists available at ScienceDirect

Journal of CO2 Utilization

journal homepage: www.elsevier.com/locate/jcou

Continuous electroreduction of CO_2 towards formate in gas-phase operation at high current densities with an anion exchange membrane

Guillermo Díaz-Sainz *, Manuel Alvarez-Guerra, Angel Irabien

Chemical and Biomolecular Engineering Department, University of Cantabria, ETSIIT, Avda. Los Castros s/n, 39005, Santander, Spain

ARTICLE INFO

Keywords:
Continuous CO_2electroreduction
Sustainion anion exchange membrane
Formate
Current density
Filter-press electrochemical reactor

ABSTRACT

The carbon dioxide (CO_2) electroreduction to formate is nowadays considered as a promising approach to convert CO_2 into a value-added product and simultaneously, in the context of strategies for mitigating climate change. However, there is a scarce number of studies published in the literature operating with a current density higher than 200 mA cm^{-2}, and there is the need of operating at higher current densities, with acceptable performance and low penalty in terms of energy consumption, for future implementation at industrial scale. Thus, in this work, a novel configuration is studied using a filter press reactor in a continuous mode, with a single pass of the reactants through the cell, employing a Sustainion anion exchange membrane and working with a current density up to 600 mA cm^{-2}. Using the same electrocatalysts, the configuration shows a similar performance to the GDE configuration with liquid electrolyte, but with the advantage of operating only with a vapour input to the cathode and avoiding the need for a liquid catholyte. Although at the expense of obtaining a more diluted product, excellent combinations of Faradaic Efficiency for formate (73.7 %), energy consumptions (342 kWh·$kmol^{-1}$), and product rates (22.9 mmol m^{-2}·s^{-1}) can be achieved at high current densities. Therefore, the configuration with Sustainion membranes reported in this manuscript can be particularly interesting for future applications that do not involve a very concentrated formate product.

1. Introduction

Anthropogenic actions have caused a dramatic increase in carbon dioxide (CO_2) emissions into the environment and particularly, to the atmosphere [1]. In this sense, the concentration of CO_2 has recently exceeded the threshold of 415 ppm, registered by the National Oceanic and Atmospheric Administration (NOAA) [2]. Thus, the main consequence of this gas in the atmosphere is the phenomenon commonly known as the greenhouse effect, which is the main responsible for climate change, internationally recognized by the Intergovernmental Panel on Climate Change (IPCC) [3] and by the United Nations (UN) [4]. Besides, the World Health Organization suggests that improving the environmental conditions of the atmospheric media will contribute to the population to approach in better terms against the presence of new viral infections like the SARs-CoV-2 virus, which causes the COVID-19 disease [5,6].

For this purpose, several strategies have recently been adopted for reducing the CO_2 releases into the atmosphere, and particularly, for mitigating climate change [7]. Thus, carbon capture, storage, and utilization (CCSU) has appeared as a promising strategy since it permits converting atmospheric CO_2 into value-added chemical products by thermal, photocatalytic, biochemical, chemo-enzymatic, or electrochemical approaches [8–10]. In this context, the electrochemical conversion of CO_2 into various products allows the storage of intermittent and renewable sources of energy in the form of chemicals [11,12], such as carbon monoxide [13], methane [14], alcohols [15], ethylene [15] and formic acid or formate [16,17]. Among these chemicals, formic acid or formate are considered interesting products since they could be used as a raw material in several industries or areas, as silage and animal food, leather, rubber, and pharmaceuticals and crop protection agents, among others [18]. In addition, these chemicals are also considered promising for fuel cell applications [19] and for the hydrogen storage [20].

In this context, there is a large number of studies published recently in the field of the CO_2 electroreduction towards formic acid and formate operating in a discontinuous mode in different electrochemical reactor configurations, and working mainly with Sn e.g. [21–25] and Bi-based materials e.g [26–30]. as electrocatalysts. However, most of the

* Corresponding author.
E-mail address: diazsg@unican.es (G. Díaz-Sainz).

https://doi.org/10.1016/j.jcou.2021.101822
Received 22 October 2021; Received in revised form 16 November 2021; Accepted 22 November 2021
Available online 29 November 2021

Table 1
Summary of the experimental conditions and main results reported in literature for the electrocatalytic reduction of CO_2 to obtain formic acid or formate in a continuous mode of operation with a supply of current densities higher than 200 mA·cm^{-2}. (Abbreviations: AEM: Anion Exchange Membrane, CEM: Cation Exchange Membrane, BPM: Bipolar Membrane).

Feeding in the cathode compartment	Separator	Current density (mA cm^{-2})	Faradaic Efficiency for formate (%)	References
CO_2 + liquid electrolyte	Fumasep FAB-PK-130	1000	93	[38]
CO_2 + liquid electrolyte	AEM	1000	93	[39]
CO_2 + liquid electrolyte	Nafion 117	1000	75	[40]
CO_2 + liquid electrolyte	Nafion 1100	815	83	[41]
CO_2 + liquid electrolyte	Nafion	500	91	[42]
CO_2 + liquid electrolyte	BPM	500	>90	[43]
CO_2 + liquid electrolyte	Nafion 117	500	23	[44]
CO_2 + liquid electrolyte	Selemion	471	94.2	[45]
CO_2 humidified	AEM and Nafion 115	464	97	[46]
CO_2 + liquid electrolyte	FAA-3	462	91.1	[47]
CO_2 + liquid electrolyte	(-)	450	~50	[48]
CO_2 + liquid electrolyte	FAA-3-PK-130	405	89	[49]
CO_2 + liquid electrolyte	Nafion 117	388	80	[50]
CO_2 + liquid electrolyte	Nafion 212	385 ± 19	>70	[51]
CO_2 + liquid electrolyte	Nafion 117	383	87	[52]
CO_2 + liquid electrolyte	Nafion	360.30	~0	[53]
CO_2 + liquid electrolyte	(-)	345	95	[54]
CO_2 + liquid electrolyte	Nafion 117	310	63	[55]
CO_2 + liquid electrolyte	Nafion 117	300	70	[56]
CO_2 + liquid electrolyte	CEM	300	98	[57]
CO_2 + liquid electrolyte	Nafion 212	260	94	[58]
CO_2 + liquid electrolyte	Nafion 115	250	92	[59]
CO_2 humidified	Nafion 324 & Sustainion	250	74.9	[60]
CO_2 + liquid electrolyte	Selemion	210	98	[61]
CO_2 + liquid electrolyte	Nafion 212	208	93	[62]
CO_2 + liquid electrolyte	Nafion 117	200	~80	[63]
CO_2 humidified	Nafion 117	200	46	[64]
CO_2 humidified	Nafion 117	200	25	[65]
CO_2 + liquid electrolyte	Nafion 117	200	55	[66]
CO_2 + liquid electrolyte	Nafion	200	90	[67]
CO_2 + liquid electrolyte	(-)	200	>90	[68]
CO_2 + liquid electrolyte	Nafion 324	200	98	[69]
CO_2 + liquid electrolyte	BPM	200	100	[70]
CO_2 humidified	Nafion & Sustainion	200	~80	[71]

studies work with a current density lower than the one that is considered to be required for future implementation of the electrochemical process at the industrial scale (i.e. at least 100 mA cm^{-2} [31], and even 200 mA cm^{-2} [32–34]). There are some recent efforts that have supplied high current densities, achieving promising results. In this context, it is important to note that, for example, Löwe et al., 2021 work with current densities of up to 1800 mA cm^{-2}, achieving Faradaic Efficiency for formate of approximately 70 %, but operating on a discontinuous assembled cell [35]. In order to bring the CO_2 electroreduction process closer to industrial applications, the use of a continuous electrochemical reactor is the desired operation mode [36]. Compared to discontinuous cells, continuous electrochemical reactors allow improving mass transport limitations due to the circulation of reactants and products away from the electrodes. Therefore, in general, continuous operation enhances the results in terms of the Faradaic Efficiency for the target product and energy consumption [37]. In this way, Table 1 collects all the main studies reported up to date in the literature in the field of CO_2 electroreduction to formic acid and formate working with a current density higher than 200 mA cm^{-2} in a continuous electrochemical reactor. From these previous works, the highest current density applied for the electrocatalytic reduction of CO_2 to formate, operating in a continuous mode, was 1000 mA cm^{-2}, reaching Faradaic Efficiency values up to 93 % in a flow cell reactor by using $Bi_2O_2CO_3$ nanosheet [38]. Besides, Grigioni et al., 2021 reported a Faradaic Efficiency for formate of 93 % and a partial current density of 930 mA cm^{-2} by employing synthesized InP colloidal quantum dots [39]. In contrast, Bienen et al., 2019 achieved formate concentration of 0.26 M with average Faradaic Efficiency to formate of 75 %, which permits working with a current density of 1000 mA cm^{-2} [40]. On the other hand, other recent articles have achieved considerable advances in this field, reaching a partial current density of up to 677 mA cm^{-2} for formate production [41], and values of 500 mA cm^{-2} with Faradaic Efficiency for formate of 91 % in a flow cell operating for one month [42]. Besides, and operating at 500 mA cm^{-2}, Chen et al., 2020 implemented a cell for electroreduction of CO_2 with bipolar membranes, reaching Faradaic Efficiency towards formate of up to 90 % [43]. Merino-García et al., 2021 studied the continuous electroconversion of CO_2 into formate using 2 nm SnO_2 nanoparticles at 500 mA cm^{-2}, obtaining formate concentrations of 23 g·L^{-1} and at the same time, Faradaic Efficiency of 23 % [44]. Moreover, Li et al., 2020 obtained Faradaic Efficiency close to 94.2 %, achieving formate partial current densities of approximately 471 mA cm^{-2}, using a three-compartment microfluidic flow cell electrolyzer [45]. In spite of obtaining promising results in terms of Faradaic Efficiency for the formate, all these studies use a liquid medium as an electrolyte, being the process limited by the low solubility of CO_2 in an aqueous medium. Besides, the employ of a liquid catholyte presents other significant disadvantages, such as the costs of the ionic compounds usually needed in high concentrations to prepare the electrolyte, or that the need for pumping, and eventual separation, of this electrolyte.

Apart from the previous work carried out in the DePRO research group at the University of Cantabria [64,65], and some studies developed in a three-compartment electrochemical reactor [46,60,71], all the efforts have been focused on using a liquid electrolyte at the cathode side of the electrochemical reactor. In fact, the combination of a continuous operation mode with the supply of high current densities, and simultaneously, the employ of a CO_2 humidified input stream at the cathode side of the electrochemical reactor, is rarely found in this kind of studies. In addition, the type of ionic exchange membrane employed in the electrochemical reactor is a key aspect that can play an important role in the performance of the electrocatalytic reduction of CO_2 to formic acid and formate. In general, a great number of studies on this topic use a cation exchange membrane (CEM), such as Nafion 115, 117, 212, 324,

and 1110. However, in recent years, some works have been published using anion exchange membrane (AEM) [39,72], like Sustainion [46,60,71,73,74], Fumasep [38,47,49,75–77], AMI [78], and Selemion [45,61,79–82], conforming innovative electrochemical reactor configurations, but, as shown in Table 2, scarcely studied yet in comparison with CEM, and particularly, Nafion membranes. Table 2 also summarizes the main characteristics of these publications with AEMs working in a continuous mode, as well as the main figures of merit obtained that they report. The analysis of Table 2 shows that the few studies at high current densities were carried out using an input liquid electrolyte to feed the cathode compartment. Moreover, in Table 2 it is also noteworthy that, apart from the approaches that imply both the use of CEM and AEM in a three-compartment electrochemical reactor, the performance of two-compartments reactors using an AEM with only humidified CO_2 as input stream, has been scarcely explored yet. Thus, this reinforces the interest in the study of the CO_2 electroreduction to formate process employing an anion exchange membrane as separator, and simultaneously, using a CO_2 humidified input stream to the reactor and operating at high current density.

In this context, the main goal of this manuscript is to study the CO_2 electroreduction to formate in a continuous mode with a single pass of all the reactants through the filter press reactor working with a current density up to 600 mA cm^{-2}, achieving competitive results in terms of Faradaic Efficiency for formate and energy consumption per kmol of formate. The internal configuration of the electrochemical reactor employs a Sustainion anion exchange membrane as a separator of both cathodic and anodic compartments of the reactor. Besides, the proposed configuration in this study uses a CO_2 humidified input stream at the cathode side of the electrochemical reactor, avoiding the problems associated with the CO_2 solubility in the liquid electrolytes.

2. Methodology

All the experiments reported in this study for the electrocatalytic reduction of CO_2 to formate are carried out in a continuous filter press reactor with a single pass of the reactants through the electrochemical reactor. The experimental setup employed, and, particularly, the filter press reactor and electrode configurations, are detailed below in subsection 2.1 and 2.2. Finally, the analysis of both gas and liquid phases and the different figures of merit used to assess the electrochemical conversion of CO_2 to formate are defined in sections 2.3 and 2.4, respectively.

2.1. Experimental setup

Fig. 1 depicts the experimental setup used in this study for the continuous electrocatalytic reduction of CO_2 to formate operating in a gaseous phase at the cathode side of the filter press reactor.

The key element of the experimental setup is the filter press cell (Micro Flow Cell, ElectroCell, A/s), whose internal configuration is detailed in Fig. 2. Apart from the electrochemical reactor, the experimental setup includes a peristaltic pump (Watson Marlow 320, Watson Marlow Pumps Group) and tanks for the inlet and outlet of the anolyte at the anode side of the electrochemical reactor. In this way, a 1 M KOH (potassium hydroxide, 85 % purity, pharma grade, PanReac AppliChem) aqueous solution (pH 14.0) was used as the anolyte with a flow rate of 5.7 mL min^{-1}. Pure gaseous CO_2 was fed to the electrochemical cell at a constant flow rate of 200 mL min^{-1} in accordance with previous works [64,83]. On the other hand, the gaseous stream temperature, and the vapor flow in the CO_2 input stream at the cathode side of the reactor are controlled and adjusted by a Vapour Delivery Module (VDM) (Bronkhorst, SW-200). In this sense, the experiments were conducted at room temperature (20 °C), and with an input water/CO_2 molar ratio per geometric area of 56.1 mol water·(mol CO_2)$^{-1}$ m^{-2}, since they were obtained in previous studies as the best conditions for carrying out the electroreduction of CO_2 [64,83]. Thus, these operating conditions were chosen to make a rigorous comparative assessment with previous results obtained in the DePRO research group at the University of Cantabria with others filter press reactor configurations. Both temperature and water flow were measured in the CO_2 input stream of the electrochemical reactor employing a HygroFlex HF5 humidity temperature transmitter. The pressure was also measured in the input and the output of the electrochemical cell by different pressure transmitters. Finally, all the tests were executed at galvanostatic conditions, with the current supplied by the potentiostat-galvanostat (Arbin Instruments, MSTAT4).

2.2. Filter press reactor configuration

Fig. 2 illustrates the electrochemical reactor configuration employed in this study for the continuous electrocatalytic reduction of CO_2 to formate with a single pass of the reactants through the reactor.

The key elements in the electrochemical reactor are the working electrode or cathode (number 9, Fig. 2), the counter electrode or anode (number 4, Fig. 2), the reference electrode (number 5, Fig. 2), and the ion exchange membrane (number 7, Fig. 2). The internal components of

Table 2
Main characteristics and figures of merit reported in studies in the literature that involve the use of anion exchange membranes in the field of CO_2 electroreduction to formic acid or formate operating in a continuous mode. (Abbreviations: ND: not defined).

Type of AEM membrane	Electrochemical reactor configuration	Feeding in the cathode compartment	Current density (mA cm^{-2})	Faradaic Efficiency for formate (%)	Year	References
FAA-3-PK- 130flow	Flow cell	CO_2 + liquid electrolyte	56.6	98.3	2022	[75]
Fumasep FAB-PK-130	Flow cell	CO_2 + liquid electrolyte	1000	93	2021	[38]
ND	Flow cell	CO_2 + liquid electrolyte	1000	93.1	2021	[39]
Sustainion	Flow cell	CO_2 pre-humidified	238	92.2	2021	[73]
ND	Flow cell	CO_2 + liquid electrolyte	83	92	2021	[72]
Selemion	Three-compartment Microfluidic	CO_2 + liquid electrolyte	471	94.2	2020	[45]
AEM and Nafion 115	Three-compartment	CO_2 humidified	464	97	2020	[46]
FAA-3	Flow cell	CO_2 + liquid electrolyte	462	91.1	2020	[47]
FAA-3-PK-130	Flow cell	CO_2 + liquid electrolyte	405	89	2020	[49]
Sustainion	Three-compartment	CO_2 humidified	250	74.9	2020	[60]
Selemion	Flow cell	CO_2 + liquid electrolyte	210	98	2019	[61]
Sustainion	Three-compartment	CO_2 humidified	200	~80	2019	[71]
Selemion	Flow cell	CO_2 + liquid electrolyte	18.9	82	2019	[82]
Selemion	Flow cell	CO_2 + liquid electrolyte	~9	21.1	2019	[80]
Fumatech	Flow cell	CO_2 + liquid electrolyte	145	64	2018	[76]
Selemion	Flow cell	CO_2 + liquid electrolyte	~18	100	2018	[81]
FAD	Flow cell	CO_2 + liquid electrolyte	~10	90.1	2018	[77]
Sustainion	Three-compartment	CO_2 humidified	140	94	2017	[74]
Selemion	Flow cell	CO_2 + liquid electrolyte	~6	80	2017	[79]
AMI	Flow cell	CO_2 + liquid electrolyte	40	80	2011	[78]

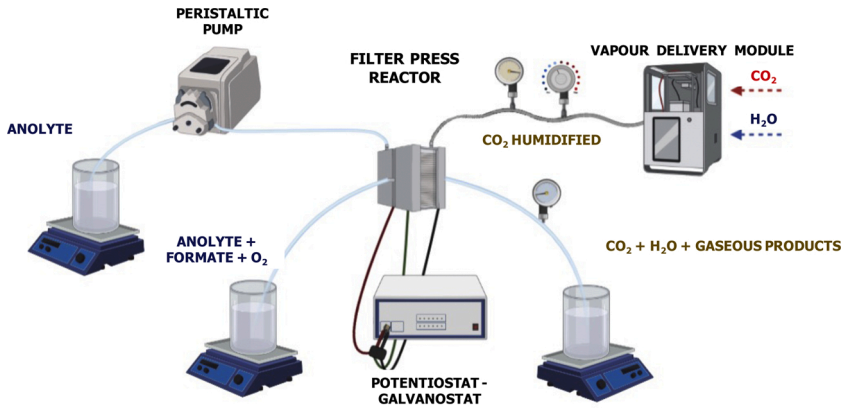

Fig. 1. Experimental setup employed for the electrocatalytic reduction of CO_2 to obtain formate operating in a gaseous phase at the cathode side of the filter press reactor.

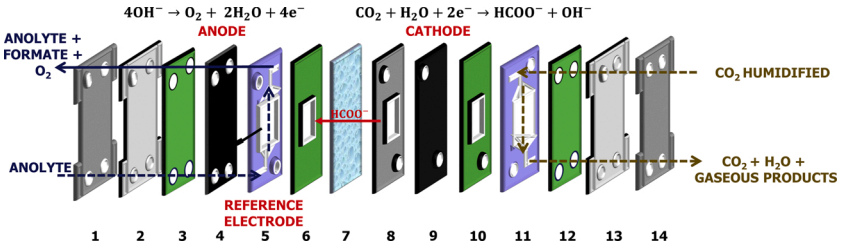

Fig. 2. Filter press cell configuration used for the continuous CO_2 electrocatalytic reduction to obtain formate operating in a gaseous phase at the cathode side of the filter press reactor (numbers 1 and 14: endplates; numbers 2 and 13: plates for tubing connection, numbers 3, 6, 10 and 12: gaskets, number 4: counter electrode, number 5: flow distributors and reference electrode, number 7: anion exchange membrane, number 8: current collector, number 9: working electrode and number 11: flow distributor).

the filter press electrochemical reactor used in this manuscript are illustrated in figure S1 of the Supporting Information. Moreover, all the tests were developed with the same carbon-supported Bi nanoparticles, whose synthesis procedure and characterization are detailed in Avila-Bolivar et al., 2019 [84]. In addition, Gas Diffusion Electrodes (GDEs) were used as cathodes in the filter-press reactor, with a Bi catalyst loading of 0.75 mg cm^{-2} (Bi/C-GDE). The GDEs were prepared following the procedure detailed in [56,65]. Moreover, a commercial dimensionally stable anode [DSA/O_2 (Ir-MMO [mixed metal oxide] on platinum), Electrocell] was used in the electrochemical filter-press reactor. As reference electrode, a leak-free Ag/AgCl 3.4 M KCl was also placed in the anodic compartment. It is important to emphasize that, in the configuration studied in this work, both compartments are separated by an anion exchange membrane, Sustainion® X37−50 Grade RT (Dioxide Materials), which allows formate to cross from the cathodic to the anodic compartment. The membranes were soaked in a large bath of 1 M KOH to activate them into the hydroxide form before their use.

As can be seen in Figs. 2 and 3, a Bi/C-MEA configuration was chosen for the electrocatalytic reduction of CO_2 to formate. In this context, the Bi/C-GDE (number 9, Fig. 2) is in contact with the anion exchange membrane (number 7, Fig. 2). Besides, the current collector (number 8, Fig. 2) is located directly between the GDE and the Sustainion anion exchange-membrane.

2.3. Gas and liquid phases analysis

The experimental setup was arranged to allow the analysis of both liquid and gas phases in the output streams of the electrochemical reactor. The gas phase in the output stream at the cathode side of the electrochemical was detected using a 4-channel micro gas chromatograph (490, Micro GC, Agilent Technologies). As carrier gases, helium (He) and argon (Ar) were used (99.99 % purity). Only hydrogen (H_2) and carbon monoxide (CO) were detected. These gases were separated in a molecular sieve 5 Å column (10 m MS5A Hi-BF SP1 pre-column).

No liquid was collected at the cathode side, so liquid only went out of the electrochemical reactor in the output stream at the anode side. This liquid stream was analyzed using an ion chromatograph (Dionex ICS 1100) equipped with an AS9−HC column, using a solution of 4.5 mmol·L^{-1} of sodium carbonate (Na_2CO_3) as the eluent at a flow rate of 1 mL min^{-1}.

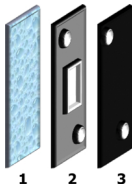

Fig. 3. Bi/C-MEA configuration used for the continuous CO_2 electrocatalytic reduction to give formate operating in a gaseous phase at the cathode side of the filter press reactor (numbers 1: Sustainion anion exchange-membrane; numbers 2: current collector and, numbers 3: Bi/C-GDE).

2.4. Figures of merit

All the experiments had a duration of time of 90 min and were performed at least in duplicate under the same operating conditions. Samples of the output streams were taken every 30 min to analyze both the liquid and gas phases, and the average value of the concentrations of each detected product was obtained for each experiment. Apart from the concentration of each product and the current density supplied to the electrochemical reactor, the performance of the electrochemical process is assessed by the Faradaic efficiency as well as the rate and energy consumption per kmol of formate. The different equations used to calculate these performance criteria can be found elsewhere [83].

3. Results

3.1. Electrochemical performance with sustainion membranes

The electrocatalytic reduction of CO_2 to formate was tested in a continuous mode employing a filter press reactor with a CO_2 humidified input stream at the cathode side, an aqueous 1 M KOH solution as an

anolyte, and a Sustainion anion exchange-membrane as a separator of the anodic and cathodic compartments. In this section, the experiments were carried out at current densities of 90, 200, and 300 mA cm^{-2}, a water/CO_2 molar ratio in the feed per geometric area of 56.1 mol water·(mol CO_2)$^{-1}$ m^{-2}, which corresponds to a water flow of 0.5 g h^{-1}, and a Bi catalyst loading of 0.75 mg cm^{-2}.

Fig. 4 shows the influence of the current density on the formate rate and on the Faradaic Efficiency for formate (specific values for all the experiments of the manuscript are reported in Table S1 of the Supplementary Information). Firstly, working with a current density of 90 mA cm^{-2}, excellent values of 95.2 % in terms of Faradaic Efficiency towards formate are achieved. However, it should be noted that increasing the current density from 90 to 300 mA cm^{-2}, the Faradaic Efficiency for formate only decreased by 4 %, achieving values of 91.6 % at 300 mA cm^{-2}. These results show that there is hardly any negative influence of the current density operating in the range between 90 and 300 mA cm^{-2}, achieving similar results in terms of the Faradaic Efficiency for formate. Regarding the formate rate, operating with a current density of 200 and 300 mA cm^{-2}, this figure of merit shows increments of 117 % (9.6 mmol m^{-2}·s^{-1}) and 220 % (14.2 mmol m^{-2}·s^{-1}), respectively, when compared to the supply of a current density of 90 mA cm^{-2}.

The concentration of the product of interest has the same trend as the formate rate mentioned previously, as depicted in Fig. 5 (values are provided in Table S1 of the Supporting Information). A formate concentration of 2.1 g·L^{-1} was obtained working at a current density of 90 mA cm^{-2}. Rising the current density to 200 and 300 mA cm^{-2}, the formate concentration reaches values of 4.5 and 6.7 g·L^{-1}, respectively, which represents a practically linear increase. Finally, and as expected, the energy consumption gets worse when the current density is increased, obtaining values of 211 kWh·$kmol^{-1}$ for 300 mA cm^{-2} (Fig. 5). Nevertheless, it is important to highlight that consumptions of less than 200 kWh·$kmol^{-1}$ were achieved for current densities of 90 al 200 mA cm^{-2} (i.e. values of only 152, and 196 kWh·$kmol^{-1}$, respectively). These remarkably low energy consumptions could be attributed to the low values of the absolute cell potentials, 3.4 V and 3.6 V, achieved at a current density of 200 mA cm^{-2} and 300 mA cm^{-2}, respectively.

Fig. 6 summarizes the Faradaic Efficiencies of all the products detected in the analysis of both the liquid and the gas phases in the output stream of the electrochemical reactor (more information is available in Table S2 of the Supplementary Information). As can be seen, apart from formate, only hydrogen and traces of carbon monoxide have been detected in all experiments carried out, reaching in all of these tests values of accumulated Faradaic Efficiency close to 100 %. The Faradaic Efficiency towards hydrogen is 4.5, 6.1, and 8.3 %, when the current

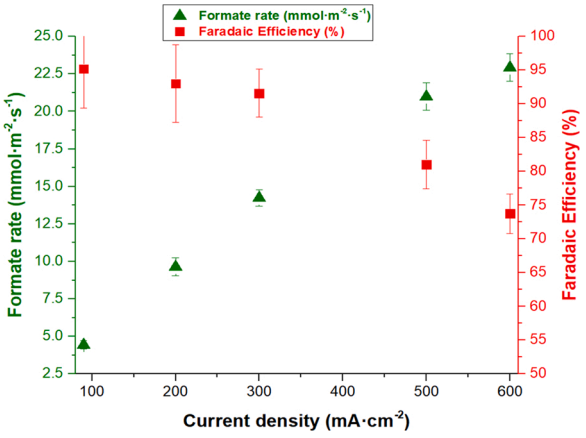

Fig. 4. Influence of current density on the formate rate (mmol·m^{-2}·s^{-1}) and Faradaic Efficiency for formate (%) in the current density range of 90 – 600 mA·cm^{-2} applied at room temperature = 20 °C, Bi Catalyst loading = 0.75 mg·cm^{-2}, and a water/CO_2 molar ratio in the feed per geometric area of 56.1 mol water·(mol CO_2)$^{-1}$ m^{-2}, using Sustainion anion exchange-membrane.

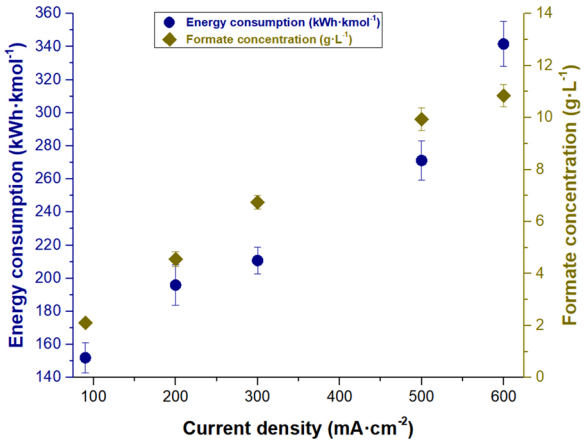

Fig. 5. Influence of current density on the energy consumption (kWh·$kmol^{-1}$) and formate concentration (g·L^{-1}) in the current density range of 90 – 600 mA·cm^{-2} applied at room temperature = 20 °C, Bi Catalyst loading = 0.75 mg·cm^{-2}, and a water/CO_2 molar ratio in the feed per geometric area of 56.1 mol water·(mol CO_2)$^{-1}$ m^{-2}, using Sustainion anion exchange-membrane.

density supplied to the electrochemical reactor is 90, 200, and 300 mA cm^{-2}, respectively. Thus, these results demonstrated an upward trend as current density increases, as is clearly illustrated in Fig. 6, verifying the tendencies reported in the literature [44,85].

3.2. Comparison with other configurations using Bi electrocatalysts and Nafion membranes

In this section, the performance of the CO_2 electroreduction to formate process using a Sustainion membrane is compared with respect to processes employing a Nafion cation exchange-membrane as a separator of cathodic and anodic compartments in different filter press reactor configurations: Bi/C-GDE [56], Bi/C−CCME [83], and Bi/C-MEA [65]. Table 3 compares the main results achieved in this work with those obtained using a Nafion membrane in the different configurations indicated above. In this sense, Table 3 is divided according to the current density supplied to the electrochemical reactor: 90−100, 200,

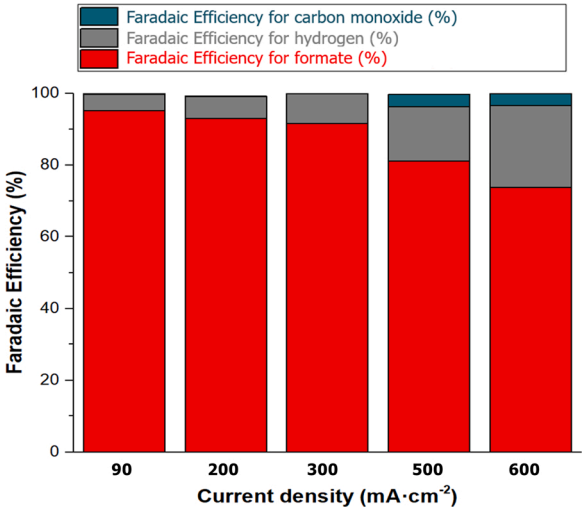

Fig. 6. Influence of current density on the Faradaic Efficiency towards formate (represented in red color), the Faradaic Efficiency towards hydrogen (represented in grey color), and the Faradaic Efficiency towards carbon monoxide (represented in green color) in the current density range of 90 – 600 mA·cm^{-2} applied at room temperature = 20 °C, Bi Catalyst loading = 0.75 mg·cm^{-2}, and a water/CO_2 molar ratio in the feed per geometric area of 56.1 mol water·(mol CO_2)$^{-1}$ m^{-2}, using Sustainion anion exchange-membrane.

and 300 mA cm^{-2} to make a rigorous comparative assessment. Besides, all experiments were carried out with the same carbon-supported Bi nanoparticles [84], with Bi catalyst loading of 0.75 mg cm^{-2}, and room conditions of temperature of 20 °C.

Firstly, working at a current density of 90–100 mA·cm^{-2} the results of formate concentration, Faradaic Efficiency and formate rate achieved with a Sustainion membrane configuration are slightly better than those obtained with the configuration Bi/C-GDEs. In this context, the energy consumption is clearly improved by 15 % when Sustainion membranes are used with respect to Nafion. This improvement in the energy consumption is mainly due to the lower values of absolute cell potential observed (2.7 V), compared to 3.1 V, obtained with the Bi/C-GDE configuration. In view of these results, it is important to emphasize that the configuration studied in this manuscript employs only a humidified CO_2 input stream at the cathode side of the filter press reactor, achieving similar results as the Bi/C-GDEs configuration that implies using a catholyte solution of 0.5 M KCl + 0.45 M $KHCO_3$, and avoiding the use of this liquid electrolyte. In contrast, in spite of obtaining formate concentrations of 33.5 g·L^{-1} working with the Bi/C−CCME configuration, both Faradaic Efficiency and the formate rate decrease approximately 50 %. Regarding energy consumption, this figure of merit also gets worse in the Bi/C−CCME configuration, increases by more than 100 % when compared to the value obtained in the current work. This phenomenon also occurs with the Bi/C-MEA configuration, where competitive values of formate concentration were obtained (256 g·L^{-1}), but at the expense of achieving worse values in terms of Faradaic Efficiency for formate (40.5 %), formate rate (2.1 mmol m^{-2}·s^{-1}) and energy consumption (409 kWh·$kmol^{-1}$).

The same comparative assessment can be carried out for a current density of 200 mA cm^{-2}. The improvement of the process observed using a Sustainion membrane with respect to the use of a Nafion membranes in the Bi/C-GDE configuration is enhanced increasing the current density to 200 mA cm^{-2}. As can be seen in Table 3, the values of formate concentration, Faradaic Efficiency and formate rate are 15 % higher than those obtained with the GDE configuration [56]. The reduction in energy consumption with Sustainion membranes is particularly remarkable, achieving a value of only 196 kWh·$kmol^{-1}$, approximately 30 % lower. Furthermore, it is important to highlight again that the better results in this study using a Sustainion membrane than those in the Bi/C-GDE configuration were achieved with a CO_2 humidified input stream to the cathodic compartment of the electrochemical reactor, removing the use of the liquid electrolyte in this compartment. This possibility would represent a clear advantage in processes for the production of formate by CO_2 electroreduction. A CO_2 humidified input stream is also used in both Bi/C−CCME and Bi/C-MEA configurations, reaching values of formate concentrations of 43.2 and 312 g·L^{-1}, respectively, but at the expense of achieving much worse values in terms of Faradaic Efficiency (42.8 and 24.8 %, respectively), formate rate (2.8 and 2.6 mmol m^{-2}·s^{-1}, respectively) and energy consumption (434 and 547 kWh·$kmol^{-1}$, respectively).

Finally, the difference between the performance for the electrocatalytic reduction of CO_2 to formate process using Sustainion and Nafion membranes is higher operating for a current density of 300 mA cm^{-2}. First, it is important to highlight previous approaches that also involved a CO_2 humidified input stream to the cathode (Bi/C−CCME [83] and Bi/C_MEA [65]) were not able to operate at such high current densities with acceptable performance. However, in the configuration employing a Sustainion membrane, both the Faradaic Efficiency, and the formate rate and concentration are approximately 30 % higher than in the Bi/C-GDE configuration, achieving values of 91.6 %, 14.2 mmol m^{-2}·s^{-1} and 6.7 g·L^{-1}, respectively (Table 3). Besides, the energy consumption obtained with Sustainion membranes is 211 kWh·$kmol^{-1}$, 48 % lower than the obtained with the Bi/C-GDEs configuration under the same operating conditions, which can be attributed to the low absolute cell potential achieved with Sustainion membranes (3.6 V), compared to those attained with Nafion membranes (5.2 V).

Table 3
Comparison of the results obtained with the Sustainion anion exchange-membrane with the previous results obtained using Nafion cation exchange-membrane in the configuration of Bi/C-GDE [56], Bi/C−CCME [83], Bi/C-MEA [65] for values of current density of 90-100, 200 and 300 mA·cm^{-2} at a Bi catalyst loading of 0.75 mg·cm^{-2} and a temperature of 20 °C.

Current density of 90–100 mA·cm^{-2}							
Configuration	Catholyte flow (mL min^{-1})	Formate concentration (g·L^{-1})	Faradaic Efficiency for formate (%)	Formate rate (mmol m^{-2}·s^{-1})	Energy consumption (kWh·$kmol^{-1}$)	Absolute cell potential (V)	Standard deviation (%)
Sustainion	~0.008 (0.5 g h^{-1})	2.1	95.2	4.4	152	2.7	6.0
Bi/C-GDE [56]	5.7	2.0	92.4	4.3	177	3.1	7.2
Bi/C-CCME [83]	~0.008 (0.5 g h^{-1})	33.5	50.2	2.3	322	3.0	9.7
Bi/C-MEA [65]	~0.008 (0.5 g h^{-1})	256	40.5	2.1	409	3.1	3.3
Current density of 200 mA cm^{-2}							
Configuration	Catholyte flow (mL min^{-1})	Formate concentration (g·L^{-1})	Faradaic Efficiency for formate (%)	Formate rate (mmol m^{-2}·s^{-1})	Energy consumption (kWh·$kmol^{-1}$)	Absolute cell potential (V)	Standard deviation (%)
Sustainion	~0.008 (0.5 g h^{-1})	4.5	93.0	9.6	196	3.4	6.2
Bi/C-GDE [56]	5.7	3.9	80.4	8.3	277	4.2	1.8
Bi/C-CCME [83]	~0.008 (0.5 g h^{-1})	43.2	42.8	2.8	434	3.5	5.1
Bi/C-MEA [65]	~0.008 (0.5 g h^{-1})	312	24.8	2.6	547	3.8	2.7
Current density of 300 mA cm^{-2}							
Configuration	Catholyte flow (mL min^{-1})	Formate concentration (g·L^{-1})	Faradaic Efficiency for formate (%)	Formate rate (mmol m^{-2}·s^{-1})	Energy consumption (kWh·$kmol^{-1}$)	Absolute cell potential (V)	Standard deviation (%)
Sustainion	~0.008 (0.5 g h^{-1})	6.7	91.6	14.2	211	3.6	3.9
Bi/C-GDE [56]	5.7	5.2	70.6	11.0	410	5.2	2.6

Table 4
Performance of different types of the membrane in terms of area-specific resistance under a different pH range. Data taken from [86].

Membrane	Area-specific resistance ($\Omega \cdot cm^2$)	pH range
Sustainion® 37−50	0.045	2−14
Nafion 115	0.52	0−13
Fumasep FAPQ-375	0.83	0−11
AMI-7001	2	0−10
PBI	8.3	2−10
Neosepta ACN	>50	0−8

3.3. Further improvements at high current densities

As a consequence of the competitive results obtained in terms of formate concentration, Faradaic Efficiency, formate rate and particularly, energy consumption, for a current density of 300 mA cm^{-2}, discussed in section 3.1, further experiments were carried out at higher current densities: 500 and 600 mA cm^{-2}. These tests were developed working with a Bi catalyst loading of 0.75 mg cm^{-2}, and a ratio of water moles of CO_2 in the feed per geometric area of 56.1 mol water·(mol CO_2)$^{-1}$ m^{-2},which corresponds to a water flow in the CO_2 input stream of 0.5 g h^{-1}. The results obtained operating under these high current densities are included in Figs. 4–6.

Firstly, operating with a current density of 500 mA cm^{-2}, formate concentrations, Faradaic Efficiency, formate rate and energy consumption of 9.9 g·L^{-1}, 81 %, 21 mmol m^{-2}·s^{-1} and 271 kWh·$kmol^{-1}$, respectively, were reached. Both the formate concentration and the rate present an increase of approximately 50 %, with respect to the operation using a current density of 300 mA cm^{-2}. However, in spite of obtaining excellent Faradaic Efficiencies and energy consumption values at 500 mA cm^{-2}, both figures of merit worsened by 11.5 and 28.7 %, respectively, compared to the supply of a current density of 300 mA cm^{-2}.

Moreover, when the current density supplied is 600 mA cm^{-2}, the trends of the different figures of merit are the same as described previously for the current density of 500 mA cm^{-2}. Thus, both formate concentration and the formate rate are increased by 10 %, while the Faradaic Efficiency towards formate and energy consumption worsens by the same percentage, with an increase in the current density from 500 to 600 mA cm^{-2}. In this sense, formate concentrations, Faradaic efficiencies, production speeds and energy consumption of 10.8 g·L^{-1}, 73.7 %, 22.9 mmol m^{-2}·s^{-1} and 341 kWh·$kmol^{-1}$, respectively, are obtained.

Besides, Fig. 6 represents the results obtained from the analysis of the phase gaseous for the experiments at 500 and 600 mA cm^{-2}. On the one hand, the Faradaic Efficiency towards hydrogen reaches values of 15.2 and 22.8 % when working at 500 and 600 mA cm^{-2}, respectively, showing a higher production of hydrogen with an increase in the current density. In contrast, carbon monoxide remains as a minor product, achieving Faradaic Efficiency of approximately 3.4 %, when operating at 500 and 600 mA cm^{-2}, respectively.

In general, the competitive values in: (i) Faradaic Efficiency for formate, (ii) formate rate, and (iii) the energy consumption per kmol of formate could be attributed to the fact that the Sustainion anion exchange-membranes exhibits an excellent performance and has a very low area-specific resistance under alkaline conditions (0.045 $\Omega \cdot cm^2$, Table 4) as a consequence of the anolyte used (aqueous 1 M KOH solution). Moreover, according to data obtained from the manufacturer (Dioxide Materials), the conductivity of Sustainion® X37−50 Grade RT in 1 M KOH is 116 mS·cm^{-1}, with a thickness after activation of only 74 μm. It is also important to note that, at the same pH conditions, the resistance of Sustainion® anion exchange-membrane is more than an order lower than other types of membranes, such as Nafion cation exchange-membranes, employed in previous works (Table 4).

4. Conclusions

The novel configuration studied in this work involves the use of a Sustainion anion exchange-membrane to separate the cathodic and anodic compartments of a filter press electrochemical reactor operating in a continuous mode with a single pass of the reactants through the cell for the electrocatalytic reduction of CO_2 to formate. The configuration studied shows a similar performance to the GDE configuration with a liquid electrolyte, but with the advantage of operating only CO_2 with vapour water as an input to the cathode and removing the necessity of a liquid catholyte such as the solution of KCl + $KHCO_3$ typically used as catholyte with GDEs.

In this sense, competitive results and excellent combinations of Faradaic efficiency for formate, energy consumption, and product rates can be achieved, at the expense of obtaining a more diluted product. Therefore, the configuration with the Sustainion membrane studied through this manuscript can be particularly interesting for future applications that do not involve a very concentrated formate product.

As could be expected, increasing the current density when operating with this configuration turns into a decrease in the performance of the process. Nevertheless, interestingly, unlike most previous approaches, in the configuration presented there is hardly any deterioration of the Faradaic Efficiency towards formate when increasing the current density to high values of 300 mA cm^{-2}. In addition, these results present a significant advance in the field of CO_2 electroreduction to formate due to obtaining competitive values of Faradaic Efficiency (73.7 %) and energy consumption (341 kWh·$kmol^{-1}$), with a supply of current densities of up to 600 mA cm^{-2} (or electric current of 6 A) in a continuous filter press reactor, bringing this process closer for future implementation at the industrial scale.

CRediT authorship contribution statement

Guillermo Díaz-Sainz: Investigation, Methodology, Data curation, Writing - original draft, Writing - review & editing, Visualization. **Manuel Alvarez-Guerra:** Methodology, Conceptualization, Writing - review & editing, Visualization, Supervision, Project administration, Funding acquisition. **Angel Irabien:** Conceptualization, Writing - review & editing, Supervision, Project administration, Funding acquisition.

Declaration of Competing Interest

The authors report no declarations of interest.

Acknowledgments

Authors fully acknowledge the financial support received from the Spanish State Research Agency (AEI) through the projects PID2019-108136RB-C31 (AEI/10.13039/501100011033) and PID2020-112845RB-I00 (AEI/10.13039/501100011033). We are also grateful for the nanoparticles prepared and provided by the group of Prof. V. Montiel and Dr. José Solla-Gullón from the Institute of Electrochemistry of the University of Alicante. The authors also thank BioRender.com online software as this science illustration tool has allowed to create some of the figures of this manuscript.

Appendix A. Supplementary data

Supplementary material related to this article can be found, in the online version, at doi:https://doi.org/10.1016/j.jcou.2021.101822.

References

[1] United States Environmental Protection Agency, Overview of Greenhouse Gases, 2021 (Accessed 16 November, 2021), https://www.epa.gov/ghgemissions/overview-greenhouse-gases#carbon-dioxide.
[2] National Oceanic and Atmospheric Administration, U.S. Department of Commerce, 2021 (Accessed 16 November, 2021), https://www.noaa.gov/.

[3] The Intergovernmental Panel on Climate Change, 2021 (Accessed 16 November, 2021), https://www.ipcc.ch/.

[4] Objetivos de desarrollo sostenible, 2021 (Accessed 16 November, 2021), https://www.un.org/sustainabledevelopment/es/objetivos-de-desarrollo-sostenible/.

[5] M. Urrutia-Pereira, C.A. Mello-da-Silva, D. Solé, COVID-19 and air pollution: A dangerous association? Allergol. Immunopathol. (Madr). 48 (2020) 496–499, https://doi.org/10.1016/j.aller.2020.05.004.

[6] Organización Mundial de la Salud, 2021 (Accessed 16 November, 2021), https://www.who.int/es.

[7] A. Irabien, M. Alvarez-Guerra, J. Albo, A. Domínguez-Ramos, Electrochemical conversion of CO_2 to value-added products, in: C.A. Martínez-Huitle, M.A. Rodrigo, O. Scialdone (Eds.), Electrochemical Water Wastewater Treatment, Elsevier, 2018, pp. 29–59.

[8] A.D.N. Kamkeng, M. Wang, J. Hu, W. Du, F. Qian, Transformation technologies for CO_2 utilisation: current status, challenges and future prospects, Chem. Eng. J. 409 (2021), 128138, https://doi.org/10.1016/j.cej.2020.128138.

[9] J. Hyun Park, J. Yang, D. Kim, H. Gim, W. Yeong Choi, J.W. Lee, Review of recent technologies for transforming carbon dioxide to carbon materials, Chem. Eng. J. 427 (2021), 130980, https://doi.org/10.1016/j.cej.2021.130980.

[10] A. Saravanan, P. Senthil kumar, D.V.N. Vo, S. Jeevanantham, V. Bhuvaneswari, V. Anantha Narayanan, P.R. Yaashikaa, S. Swetha, B. Reshma, A comprehensive review on different approaches for CO_2 utilization and conversion pathways, Chem. Eng. Sci. 236 (2021), 116515, https://doi.org/10.1016/j.ces.2021.116515.

[11] X. Tan, C. Yu, Y. Ren, S. Cui, W. Li, J. Qiu, Recent advances in innovative strategies for the CO_2 electroreduction reaction, Energy Environ. Sci. 14 (2021) 765–780, https://doi.org/10.1039/d0ee02981e.

[12] V.C. Hoang, V.G. Gomes, N. Kornienko, Metal-based nanomaterials for efficient CO_2 electroreduction: recent advances in mechanism, material design and selectivity, Nano Energy 78 (2020), 105311, https://doi.org/10.1016/j.nanoen.2020.105311.

[13] M. Jouny, G.S. Hutchings, F. Jiao, Carbon monoxide electroreduction as an emerging platform for carbon utilization, Nat. Catal. 2 (2019) 1062–1070, https://doi.org/10.1038/s41929-019-0388-2.

[14] S.A. Mazari, N. Hossain, W.J. Basirun, N.M. Mubarak, R. Abro, N. Sabzoi, A. Shah, An overview of catalytic conversion of CO_2 into fuels and chemicals using metal organic frameworks, Process Saf. Environ. Prot. 149 (2021) 67–92, https://doi.org/10.1016/j.psep.2020.10.025.

[15] B. Zhang, B. Zhang, Y. Jiang, T. Ma, H. Pan, W. Sun, Single-Atom Electrocatalysts for Multi-Electron Reduction of CO_2, 2101443, 2021, pp. 1–17, https://doi.org/10.1002/smll.202101443.

[16] X. An, S. Li, X. Hao, Z. Xie, X. Du, Z. Wang, X. Hao, A. Abudula, G. Guan, Common strategies for improving the performances of tin and bismuth-based catalysts in the electrocatalytic reduction of CO_2 to formic acid/formate, Renew. Sust. Energy Rev. 143 (2021), 110952, https://doi.org/10.1016/j.rser.2021.110952.

[17] S.A. Al-Tamreh, M.H. Ibrahim, M.H. El-Naas, J. Vaes, D. Pant, A. Benamor, A. Amhamed, Electroreduction of Carbon Dioxide into formate: a comprehensive review, Chem. Electro. Chem. 8 (2021) 1–15, https://doi.org/10.1002/celc.202100438.

[18] D. Du, R. Lan, J. Humphreys, S. Tao, Progress in inorganic cathode catalysts for electrochemical conversion of carbon dioxide into formate or formic acid, J. Appl. Electrochem. 47 (2017) 661–678, https://doi.org/10.1007/s10800-017-1078-x.

[19] Z. Ma, U. Legrand, E. Pahija, J.R. Tavares, D.C. Boffito, From CO_2 to formic acid fuel cells, Ind. Eng. Chem. Res. 60 (2021) 803–815, https://doi.org/10.1021/acs.iecr.0c04711.

[20] J.S. Yoo, R. Christensen, T. Vegge, J.K. Nørskov, F. Studt, Theoretical insight into the trends that guide the electrochemical reduction of Carbon Dioxide to formic acid, Chem. Sus. Chem. 9 (2016) 358–363, https://doi.org/10.1002/cssc.201501197.

[21] Q. Wang, Y. Wu, C. Zhu, R. Xiong, Y. Deng, X. Wang, C. Wu, H. Yu, Sn nanoparticles deposited onto a gas diffusion layer via impregnation-electroreduction for enhanced CO_2 electroreduction to formate, Electrochim. Acta 369 (2021), 137662, https://doi.org/10.1016/j.electacta.2020.137662.

[22] G. Chen, D. Ye, R. Chen, J. Li, X. Zhu, Q. Liao, Enhanced efficiency for carbon dioxide electroreduction to formate by electrodeposition Sn on Cu nanowires, J. CO_2 Util. 44 (2021), 101409, https://doi.org/10.1016/j.jcou.2020.101409.

[23] L. Peng, Y. Wang, I. Masood, B. Zhou, Y. Wang, J. Lin, J. Qiao, F.Y. Zhang, Self-growing Cu/Sn bimetallic electrocatalysts on nitrogen-doped porous carbon cloth with 3D-hierarchical honeycomb structure for highly active carbon dioxide reduction, Appl. Catal. B Environ. 264 (2020), 118447, https://doi.org/10.1016/j.apcatb.2019.118447.

[24] H. Li, N. Xiao, Y. Wang, C. Liu, S. Zhang, H. Zhang, J. Bai, J. Xiao, C. Li, Z. Guo, S. Zhao, J. Qiu, Promoting the electroreduction of CO_2 with oxygen vacancies on a plasma-Activated SnO:X/carbon foam monolithic electrode, J. Mater. Chem. A. 8 (2020) 1779–1786, https://doi.org/10.1039/c9ta12401b.

[25] K. Ye, Z. Zhou, J. Shao, L. Lin, D. Gao, N. Ta, R. Si, G. Wang, X. Bao, In situ reconstruction of a hierarchical Sn-Cu/SnOx Core/Shell catalyst for high-performance CO_2 electroreduction, Angew. Chemie - Int. Ed. 59 (2020) 4814–4821, https://doi.org/10.1002/anie.201916538.

[26] C. Zhu, Q. Wang, C. Wu, Rapid and scalable synthesis of bismuth dendrites on copper mesh as a high-performance cathode for electroreduction of CO_2 to formate, J. CO_2 Util. 36 (2020) 96–104, https://doi.org/10.1016/j.jcou.2019.11.017.

[27] Y. Tian, D. Li, J. Wu, J. Liu, C. Li, G. Liu, D. Chen, Y. Feng, Electroreduction of CO_2 to formate with excellent selectivity and stability on nano-dendrite Bi film electrode, J. CO_2 Util. 43 (2021), 101360, https://doi.org/10.1016/j.jcou.2020.101360.

[28] F. Yang, A.O. Elnabawy, R. Schimmenti, P. Song, J. Wang, Z. Peng, S. Yao, R. Deng, S. Song, Y. Lin, M. Mavrikakis, W. Xu, Bismuthene for highly efficient carbon dioxide electroreduction reaction, Nat. Commun. 11 (2020) 1088, https://doi.org/10.1038/s41467-020-14914-9.

[29] D. Wu, X. Wang, X.Z. Fu, J.L. Luo, Ultrasmall Bi nanoparticles confined in carbon nanosheets as highly active and durable catalysts for CO_2 electroreduction, Appl. Catal. B Environ. 284 (2021), 119723, https://doi.org/10.1016/j.apcatb.2020.119723.

[30] D. Wu, W. Chen, X. Wang, X.Z. Fu, J.L. Luo, Metal-support interaction enhanced electrochemical reduction of CO_2 to formate between graphene and Bi nanoparticles, J. CO_2 Util. 37 (2020) 353–359, https://doi.org/10.1016/j.jcou.2020.02.007.

[31] P. De Luna, C. Hahn, D. Higgins, S.A. Jaffer, T.F. Jaramillo, E.H. Sargent, What would it take for renewably powered electrosynthesis to displace petrochemical processes? Science 364 (2019), eaav3506 https://doi.org/10.1126/science.aav3506.

[32] T. Burdyny, W.A. Smith, CO_2 reduction on gas-diffusion electrodes and why catalytic performance must be assessed at commercially-relevant conditions, Energy Environ. Sci. 12 (2019) 1442–1453, https://doi.org/10.1039/c8ee03134g.

[33] J.M. Spurgeon, B. Kumar, A comparative technoeconomic analysis of pathways for commercial electrochemical CO_2 reduction to liquid products, Energy Environ. Sci. 11 (2018) 1536–1551, https://doi.org/10.1039/c8ee00097b.

[34] H. Rabiee, L. Ge, X. Zhang, S. Hu, M. Li, Z. Yuan, Gas diffusion electrodes (GDEs) for electrochemical reduction of carbon dioxide, carbon monoxide, and dinitrogen to value-added products: a review, Energy Environ. Sci. 14 (2021) 1959–2008, https://doi.org/10.1039/d0ee03756g.

[35] A. Löwe, M. Schmidt, F. Bienen, D. Kopljar, N. Wagner, E. Klemm, Optimizing Reaction Conditions and Gas Diffusion Electrodes Applied in the CO_2 Reduction Reaction to Formate to Reach Current Densities up to 1.8 A $cm^{-}2$, ACS Sustain. Chem. Eng. 9 (2021) 4213–4223, https://doi.org/10.1021/acssuschemeng.1c00199.

[36] C. Oloman, H. Li, Electrochemical processing of carbon dioxide, ChemSusChem. 1 (2008) 385–391, https://doi.org/10.1002/cssc.200800015.

[37] T.P. Nicholls, C. Schotten, C.E. Willans, Electrochemistry in continuous systems, Curr. Opin. Green Sustain. Chem. 26 (2020), 100355, https://doi.org/10.1016/j.cogsc.2020.100355.

[38] T. Fan, W. Ma, M. Xie, H. Liu, J. Zhang, S. Yang, P. Huang, Y. Dong, Z. Chen, X. Yi, Achieving high current density for electrocatalytic reduction of CO_2 to formate on bismuth-based catalysts, Cell Reports Phys. Sci. 2 (2021), 100353, https://doi.org/10.1016/j.xcrp.2021.100353.

[39] I. Grigioni, L.K. Sagar, Y.C. Li, G. Lee, Y. Yan, K. Bertens, R.K. Miao, X. Wang, J. Abed, D.H. Won, F.P. Garciá De Arquer, A.H. Ip, D. Sinton, E.H. Sargent, CO_2 electroreduction to formate at a partial current density of 930 mA cm^{-2} with InP colloidal quantum dot derived catalysts, ACS Energy Lett. 6 (2021) 79–84, https://doi.org/10.1021/acsenergylett.0c02165.

[40] F. Bienen, D. Kopljar, A. Löwe, P. Aßmann, M. Stoll, P. Rößner, N. Wagner, A. Friedrich, E. Klemm, Utilizing formate as an energy carrier by coupling CO_2 electrolysis with fuel cell devices, Chemie-Ingenieur-Technik. 91 (2019) 872–882, https://doi.org/10.1002/cite.201800212.

[41] Z. Xing, X. Hu, X. Feng, Tuning the microenvironment in gas-diffusion electrodes enables high-rate CO_2 electrolysis to formate, ACS Energy Lett. 6 (2021) 1694–1702, https://doi.org/10.1021/acsenergylett.1c00612.

[42] S. He, F. Ni, Y. Ji, L. Wang, Y. Wen, H. Bai, G. Liu, Y. Zhang, Y. Li, B. Zhang, H. Peng, The p-Orbital delocalization of main-group metals to boost CO_2 electroreduction, Angew. Chemie - Int. Ed. 57 (2018) 16114–16119, https://doi.org/10.1002/anie.201810538.

[43] Y. Chen, A. Vise, W.E. Klein, F.C. Cetinbas, D.J. Myers, W.A. Smith, W.A. Smith, W. A. Smith, T.G. Deutsch, K.C. Neyerlin, A. Robust, Scalable platform for the electrochemical conversion of CO_2 to formate: identifying pathways to higher energy efficiencies, ACS Energy Lett. 5 (2020) 1825–1833, https://doi.org/10.1021/acsenergylett.0c00860.

[44] I. Merino-Garcia, L. Tinat, J. Albo, M. Alvarez-Guerra, A. Irabien, O. Durupthy, V. Vivier, C.M. Sánchez-Sánchez, Continuous electroconversion of CO_2 into formate using 2 nm tin oxide nanoparticles, Appl. Catal. B Environ. 297 (2021), 120447, https://doi.org/10.1016/j.apcatb.2021.120447.

[45] J. Li, J. Jiao, H. Zhang, P. Zhu, H. Ma, C. Chen, H. Xiao, Q. Lu, Two-Dimensional SnO_2Nanosheets for Efficient Carbon Dioxide Electroreduction to Formate, ACS Sustain. Chem. Eng. 8 (2020) 4975–4982, https://doi.org/10.1021/acssuschemeng.0c01070.

[46] L. Fan, C. Xia, P. Zhu, Y. Lu, H. Wang, Electrochemical CO_2 reduction to high-concentration pure formic acid solutions in an all-solid-state reactor, Nat. Commun. 11 (2020), 3633, https://doi.org/10.1038/s41467-020-17403-1.

[47] L.X. Liu, Y. Zhou, Y.C. Chang, J.R. Zhang, L.P. Jiang, W. Zhu, Y. Lin, Tuning Sn_3O_4 for CO_2 reduction to formate with ultra-high current density, Nano Energy 77 (2020), 105296, https://doi.org/10.1016/j.nanoen.2020.105296.

[48] A. Seifitokaldani, C.M. Gabardo, T. Burdyny, C.T. Dinh, J.P. Edwards, M.G. Kibria, O.S. Bushuyev, S.O. Kelley, D. Sinton, E.H. Sargent, Hydronium-induced switching between CO_2 electroreduction pathways, J. Am. Chem. Soc. 140 (2018) 3833–3837, https://doi.org/10.1021/jacs.7b13542.

[49] J. Yang, X. Wang, Y. Qu, X. Wang, H. Huo, Q. Fan, J. Wang, L.M. Yang, Y. Wu, Bi-based metal-organic framework derived leafy bismuth nanosheets for carbon dioxide electroreduction, Adv. Energy Mater. 10 (2020), 2001709, https://doi.org/10.1002/aenm.202001709.

[50] S. Sen, B. Skinn, T. Hall, M. Inman, E.J. Taylor, F.R. Brushett, Pulsed electrodeposition of tin electrocatalysts onto gas diffusion layers for carbon dioxide

reduction to formate, MRS Adv. 2 (2017) 451–458, https://doi.org/10.1557/adv.2016.652.
[51] S. Sen, S.M. Brown, M.L. Leonard, F.R. Brushett, Electroreduction of carbon dioxide to formate at high current densities using tin and tin oxide gas diffusion electrodes, J. Appl. Electrochem. 49 (2019) 917–928, https://doi.org/10.1007/s10800-019-01332-z.
[52] Y. Qian, Y. Liu, H. Tang, B.L. Lin, Highly efficient electroreduction of CO_2 to formate by nanorod@2D nanosheets SnO, J. CO_2 Util. 42 (2020), 101287, https://doi.org/10.1016/j.jcou.2020.101287.
[53] L. Yi, J. Chen, P. Shao, J. Huang, X. Peng, J. Li, G. Wang, C. Zhang, Z. Wen, Molten-salt-Assisted synthesis of bismuth nanosheets for long-term continuous electrocatalytic conversion of CO_2 to formate, Angew. Chemie - Int. Ed. 59 (2020) 20112–20119, https://doi.org/10.1002/anie.202008316.
[54] X. Lu, D.Y.C. Leung, H. Wang, J. Xuan, A high performance dual electrolyte microfluidic reactor for the utilization of CO_2, Appl. Energy 194 (2017) 549–559, https://doi.org/10.1016/j.apenergy.2016.05.091.
[55] H. Li, C. Oloman, Development of a continuous reactor for the electro-reduction of carbon dioxide to formate - Part 2: scale-up, J. Appl. Electrochem. 37 (2007) 1107–1117, https://doi.org/10.1007/s10800-007-9371-8.
[56] G. Díaz-Sainz, M. Alvarez-Guerra, J. Solla-Gullón, L. García-Cruz, V. Montiel, A. Irabien, CO_2electroreduction to formate: Continuous single-pass operation in a filter-press reactor at high current densities using Bi gas diffusion electrodes, J. CO2 Util. 34 (2019) 12–19, https://doi.org/10.1016/j.jcou.2019.05.035.
[57] C.J. Peng, G. Zeng, D.D. Ma, C. Cao, S. Zhou, X.T. Wu, Q.L. Zhu, Hydrangea-like superstructured micro/nanoreactor of topotactically converted ultrathin bismuth nanosheets for highly active CO_2 electroreduction to formate, ACS Appl. Mater. Interfaces 13 (2021) 20589–20597, https://doi.org/10.1021/acsami.1c03871.
[58] R. Wang, D. Qi, X. Liu, L. Zhao, S. Huang, Z. Chen, M. Chen, B. Li, Y. You, B. Pang, Yu Xia, Exfoliated ultrathin znin2s4 nanosheets with abundant zinc vacancies for enhanced co$_2$ electroreduction to formate, Chem. Sus. Chem. 430074 (2021) 852–859, https://doi.org/10.1002/cssc.202002785.
[59] Y. Xing, X. Kong, X. Guo, Y. Liu, Q. Li, Y. Zhang, Y. Sheng, X. Yang, Z. Geng, J. Zeng, Bi@Sn core–Shell structure with compressive strain boosts the electroreduction of CO_2 into formic acid, Adv. Sci. 7 (2020), 1902989, https://doi.org/10.1002/advs.201902989.
[60] H. Yang, J.J. Kaczur, S.D. Sajjad, R.I. Masel, Performance and long-term stability of CO_2 conversion to formic acid using a three-compartment electrolyzer design, J. CO_2 Util. 42 (2020), 101349, https://doi.org/10.1016/j.jcou.2020.101349.
[61] Q. Gong, P. Ding, M. Xu, X. Zhu, M. Wang, J. Deng, Q. Ma, N. Han, Y. Zhu, J. Lu, Z. Feng, Y. Li, W. Zhou, Y. Li, Structural defects on converted bismuth oxide nanotubes enable highly active electrocatalysis of carbon dioxide reduction, Nat. Commun. 10 (2019), 2807, https://doi.org/10.1038/s41467-019-10819-4.
[62] P. Deng, F. Yang, Z. Wang, S. Chen, Y. Zhou, S. Zaman, B.Y. Xia, Metal–Organic framework-derived carbon nanorods encapsulating bismuth oxides for rapid and selective CO_2 electroreduction to formate, Angew. Chemie - Int. Ed. 59 (2020) 10807–10813, https://doi.org/10.1002/anie.202000657.
[63] A. Löwe, C. Rieg, T. Hierlemann, N. Salas, D. Kopljar, N. Wagner, E. Klemm, Influence of temperature on the performance of gas diffusion electrodes in the CO_2 reduction reaction, Chem. Electro. Chem. 6 (2019) 4497–4506, https://doi.org/10.1002/celc.201900872.
[64] G. Díaz-Sainz, M. Alvarez-Guerra, J. Solla-Gullón, L. García-Cruz, V. Montiel, A. Irabien, Gas–liquid–solid reaction system for CO_2 electroreduction to formate without using supporting electrolyte, AIChE J. 66 (2020), e16299, https://doi.org/10.1002/aic.16299.
[65] G. Díaz-Sainz, M. Alvarez-Guerra, B. Ávila-Bolívar, J. Solla-Gullón, V. Montiel, A. Irabien, Improving trade-offs in the figures of merit of gas-phase single-pass continuous CO_2 electrocatalytic reduction to formate, Chem. Eng. J. 405 (2021), 126965, https://doi.org/10.1016/j.cej.2020.126965.
[66] A. Del Castillo, M. Alvarez-Guerra, J. Solla-Gullón, A. Sáez, V. Montiel, A. Irabien, Sn nanoparticles on gas diffusion electrodes: synthesis, characterization and use for continuous CO_2 electroreduction to formate, J. CO2 Util. 18 (2017) 222–228, https://doi.org/10.1016/j.jcou.2017.01.021.
[67] D. Kopljar, A. Inan, P. Vindayer, N. Wagner, E. Klemm, Electrochemical reduction of CO_2 to formate at high current density using gas diffusion electrodes, J. Appl. Electrochem. 44 (2014) 1107–1116, https://doi.org/10.1007/s10800-014-0731-x.
[68] F.P. García de Arquer, O.S. Bushuyev, P. De Luna, C.T. Dinh, A. Seifitokaldani, M. I. Saidaminov, C.S. Tan, L.N. Quan, A. Proppe, M.G. Kibria, S.O. Kelley, D. Sinton, E.H. Sargent, 2D metal oxyhalide-derived catalysts for efficient CO_2 electroreduction, Adv. Mater. 30 (2018) 6–11, https://doi.org/10.1002/adma.201802858.
[69] D. Pavesi, R.C.J. Van De Poll, J.L. Krasovic, M. Figueiredo, G.J.M. Gruter, M.T. M. Koper, K.J.P. Schouten, Cathodic Disintegration as an Easily Scalable Method for the Production of Sn-and Pb-Based Catalysts for CO_2 Reduction, ACS Sustain. Chem. Eng. 8 (2020) 15603–15610, https://doi.org/10.1021/acssuschemeng.0c04875.
[70] C. Cao, D.D. Ma, J.F. Gu, X. Xie, G. Zeng, X. Li, S.G. Han, Q.L. Zhu, X.T. Wu, Q. Xu, Metal–Organic layers leading to atomically thin bismuthene for efficient carbon dioxide electroreduction to liquid fuel, Angew. Chemie - Int. Ed. 59 (2020) 15014–15020, https://doi.org/10.1002/anie.202005577.
[71] C. Xia, P. Zhu, Q. Jiang, Y. Pan, W. Liang, E. Stavitsk, Continuous production of pure liquid fuel solutions via electrocatalytic CO_2 reduction using solid-electrolyte devices, Nat. Energy. 4 (2019) 776–785, https://doi.org/10.1038/s41560-019-0451-x.
[72] D. Wu, J. Hao, Z. Song, X.Z. Fu, J.L. Luo, All roads lead to Rome: an energy-saving integrated electrocatalytic CO_2 reduction system for concurrent value-added formate production, Chem. Eng. J. 412 (2021), 127893, https://doi.org/10.1016/j.cej.2020.127893.
[73] Z. Wang, Y. Zhou, C. Xia, W. Guo, B. You, B.Y. Xia, Efficient electroconversion of Carbon Dioxide to formate by a reconstructed amino-functionalized indium–Organic framework electrocatalyst, Angew. Chemie - Int. Ed. 60 (2021) 19107–19112, https://doi.org/10.1002/anie.202107523.
[74] H. Yang, J.J. Kaczur, S.D. Sajjad, R.I. Masel, Electrochemical conversion of CO_2 to formic acid utilizing Sustainion^{TM} membranes, J. CO2 Util. 20 (2017) 208–217, https://doi.org/10.1016/j.jcou.2017.04.011.
[75] W. Lou, L. Peng, R. He, Y. Liu, J. Qiao, CuBi electrocatalysts modulated to grow on derived copper foam for efficient CO_2-to-formate conversion, J. Colloid Interface Sci. 606 (2022) 994–1003, https://doi.org/10.1016/j.jcis.2021.08.080.
[76] C. Liang, B. Kim, S. Yang, Yang Liu, C. Francisco Woellner, Z. Li, R. Vajtai, W. Yang, J. Wu, P.J.A. Kenis, P.M. Ajayan, High efficiency electrochemical reduction of CO_2 beyond the two-electron transfer pathway on grain boundary rich ultra-small SnO_2 nanoparticles, J. Mater. Chem. A. 6 (2018) 10313–10319, https://doi.org/10.1039/c8ta01367e.
[77] T. Lei, X. Zhang, J. Jung, Y. Cai, X. Hou, Q. Zhang, J. Qiao, Continuous electroreduction of carbon dioxide to formate on Tin nanoelectrode using alkaline membrane cell configuration in aqueous medium, Catal. Today 318 (2018) 32–38, https://doi.org/10.1016/j.cattod.2017.10.003.
[78] S.R. Narayanan, B. Haines, J. Soler, T.I. Valdez, Electrochemical conversion of Carbon Dioxide to formate in alkaline polymer electrolyte membrane cells, J. Electrochem. Soc. 158 (2011), A167, https://doi.org/10.1149/1.3526312.
[79] B. Kumar, V. Atla, J.P. Brian, S. Kumari, T.Q. Nguyen, M. Sunkara, J.M. Spurgeon, Reduced SnO_2 porous nanowires with a high density of grain boundaries as catalysts for efficient electrochemical CO_2-into-HCOOH conversion, Angew. Chemie - Int. Ed. 56 (2017) 3645–3649, https://doi.org/10.1002/anie.201612194.
[80] Y.W. Choi, F. Scholten, I. Sinev, B.R. Cuenya, Enhanced stability and CO/Formate selectivity of plasma-treated SnO_x/AgO_x catalysts during CO_2 electroreduction, J. Am. Chem. Soc. 141 (2019) 5261–5266, https://doi.org/10.1021/jacs.8b12766.
[81] H. Yang, N. Han, J. Deng, J. Wu, Y. Wang, Y. Hu, P. Ding, Y. Li, Y. Li, J. Lu, Selective CO_2 reduction on 2D mesoporous Bi nanosheets, Adv. Energy Mater. 8 (2018), 1801536, https://doi.org/10.1002/aenm.201801536.
[82] J. Wang, J. Zou, X. Hu, S. Ning, X. Wang, X. Kang, S. Chen, Heterostructured intermetallic CuSn catalysts: high performance towards the electrochemical reduction of CO_2 to formate, J. Mater. Chem. A. 7 (2019) 27514–27521, https://doi.org/10.1039/c9ta11140a.
[83] G. Díaz-Sainz, M. Alvarez-Guerra, J. Solla-Gullón, L. García-Cruz, V. Montiel, A. Irabien, Catalyst coated membrane electrodes for the gas phase CO_2 electroreduction to formate, Catal. Today 346 (2020) 58–64, https://doi.org/10.1016/j.cattod.2018.11.073.
[84] B. Ávila-Bolívar, L. García-Cruz, V. Montiel, J. Solla-Gullón, Electrochemical reduction of CO_2 to formate on easily prepared carbon-supported Bi nanoparticles, Molecules. 24 (2019), 2032, https://doi.org/10.3390/molecules24112032.
[85] I. Merino-Garcia, J. Albo, A. Irabien, Tailoring gas-phase CO_2 electroreduction selectivity to hydrocarbons at Cu nanoparticles, Nanotechnology. 29 (2018), 014001, https://doi.org/10.1088/1361-6528/aa994e.
[86] Technical Information of Dioxide Materials, The CO2 Recycling CompanyTM, 2021 (Accessed 16 November, 2021), https://dioxidematerials.com/products/anion-exchange-membranes/.